Effect of residual stress due to low-velocity impact damage on the in-plane compressive strength in aluminum honeycomb sandwich panels

A. Badea, D. Wowk, and C. Marsden
Department of Mechanical and Aerospace Engineering, Royal Military College of Canada, Kingston, ON,
Tony.badea@rmc-cmr.ca, Diane.Wowk@rmc.ca, Catharine.Marsden@rmc-cmr.ca.

Abstract

Aluminum honeycomb sandwich structures are widely used in the aircraft industry in such structures as wings and fuselages due to their high stiffness-weight ratio. However, a relatively low out-of-plane resistance to indentation can lead to the formation of dents and a loss of in-plane residual strength. The standard repair manual for each aircraft specifies indentation limits due to inevitable low-velocity impacts such as hail strikes and tool drops. Compression-after-impact (CAI) loads are shown to reduce the residual strength of panels, however the driving mechanisms behind this failure mode have yet to be fully explored.

Finite element studies are carried out to determine which aspects of the impact damage are primary contributors to the reduction in residual strength in compression. Two-stage simulations involving indentation followed by compression are run to determine whether the geometric features or the residual stresses in the face sheet and crumpled core influence the peak force sustained by the panel. Preliminary results show that the presence of pre-stress is not the primary cause of the reduction in residual strength. This implies that the impact itself does not need to be simulated and that a model only containing the shape of the dent and geometry of the crumpled core may be sufficient for predicting the reduction in compressive strength in an aluminum honeycomb sandwich structure.

Introduction

Aircraft structures rely on the use of low weight and highly stiff geometries such as composite structures to meet performance goals. Such constructions typically incorporate two face sheets, a core and adhesive to bond them together. Their high stiffness-weight ratio makes them ideal for efficient aircraft designs, however their low out-of-plane resistance to indentation and susceptibility to impact damage can lead to a reduction of in-plane compressive strength. Low-velocity impacts due to such events as tool drops, hail or debris create isolated damage regions, which crush the core inside the panel and typically deform the facesheet without cracking, disbonds or punctures. This study considers barely visible impact damage (BVID) on aluminium honeycomb panels with dent depths less than 0.1”, as defined by NASA [1].

Repair or replacement of a panel is determined based on the metrics of the dent as outlined in the Structural Repair Manual (SRM) for each aircraft. The damage limits in terms of dent depth, dent area and dent diameter are conservative and are based on idealized circular dents. They do not account for features that exist on real aircraft panels such as dent location, orientation, profile, shape or groups of overlapping dents. These conservative metrics often mean that panels are repaired or replaced prematurely resulting is unnecessary downtime and cost. Having an analysis tool that could predict the strength of damaged panels in-situ, relative to its undamaged state under a variety of loading scenarios

would be extremely beneficial and could result in significant cost savings. The study presented in this paper is part of a larger project that aims to develop such an analysis tool that could be used in conjunction with 3D laser scanning to generate CAD models of the specific dent pattern that exists on each panel of the aircraft. In order to develop such a tool, a better understanding of the relationship between different damage characteristics such as the dent depth, the residual stress in the dent, the severity and depth of the crushed core on the load carrying capability of the panel is required.

While there has been research performed on the compression after impact (CAI) scenario, it has been limited to such relationships as impact energy and residual strength [2] or thicknesses of facesheets and core [3]. The FAA [4] explains that panel failure due to in-plane compression is initiated by the reduction in out-of-plane stiffness in the crumpled core at the impact site. The facesheet is less supported and the dent deepens, resulting in a reduction in load carrying capacity. Finite element models have been used to predict the peak force in compression after impact scenarios, but they have all included modeling of the impact stage [2-3] [5-6]. When dealing with aircraft that have been dented while in service, the details of the impact are unknown and the only measurable damage characteristic is the shape of the surface dent. The analysis tool should therefore be able to predict the load carrying capacity of the panel based solely off the shape of the surface dent. This requires that the relationship between the shape of the surface dent and the characteristics of the damaged core are known, as well as knowing how the damage characteristics affect the load carrying capacity of the panel.

This study focuses specifically on evaluating the role that the residual stresses in the dent region play in the compressive strength of the panel as measured by the peak in-plane compressive force the panel can withstand. This will determine whether the peak force is more dependent on the stresses or the geometry of the damaged region, which will indicate what aspects of the damage are required to be included in the analysis tool.

Approach

The most realistic approach to predicting the residual strength of the panel (peak force in compression) is to include both the low velocity impact (dent formation) and the local instability that forms due to compression of the panel in the simulation. The analysis would be split into two stages: low velocity impact (Stage 1) and Compression-After-Impact (Stage 2). Stage 1 would incorporate the deformation in the face sheet, the localized buckling of the core, the spring back once the indenter releases from the face sheet, the formation of the BVID and finally the residual stresses formed in the structure. Stage 2 would incorporate post-impact compression which would cause a local instability, grow the damaged area, initiate a kink-band propagation region and finally the global instability (panel buckling).

The proposed analysis tool would incorporate an assumed damaged state corresponding to a known dent profile and the panel would be compressed to failure while recording the force reaction versus displacement curve. The purpose of the current study is to determine whether the residual stresses in the facesheet and core need to be included in the assumed damage state. This will be accomplished by comparing the peak force predicted using the realistic approach (Stage 1 and Stage 2) to the peak force predicted from a simulation that removes the residual stresses in the facesheet and crumpled core between Stage 1 and Stage 2.

Modeling Stage 1 is done by simulating an aluminum honeycomb sandwich panel being impacted by an assumed hemispherical steel indenter. Figure 1 shows the technical drawing used to create the geometry of the model. The hemispherical indenter impacts the top face sheet at a velocity of 4 m/s, with its bottom

facesheet constrained in the vertical direction and sides of the panel constrained in-plane. The contact between the facesheets and the honeycomb core is defined to be bonded, while frictional contact between all remaining surfaces has static and dynamic frictional coefficients of 0.61 and 0.47 respectively. The honeycomb core is 5052-H34 aluminum, the face sheet is 7075-T6 aluminum and the indenter is structural steel. Their material properties are shown in Table 1, where bilinear isotropic hardening was used to model non-linearity in the aluminium.

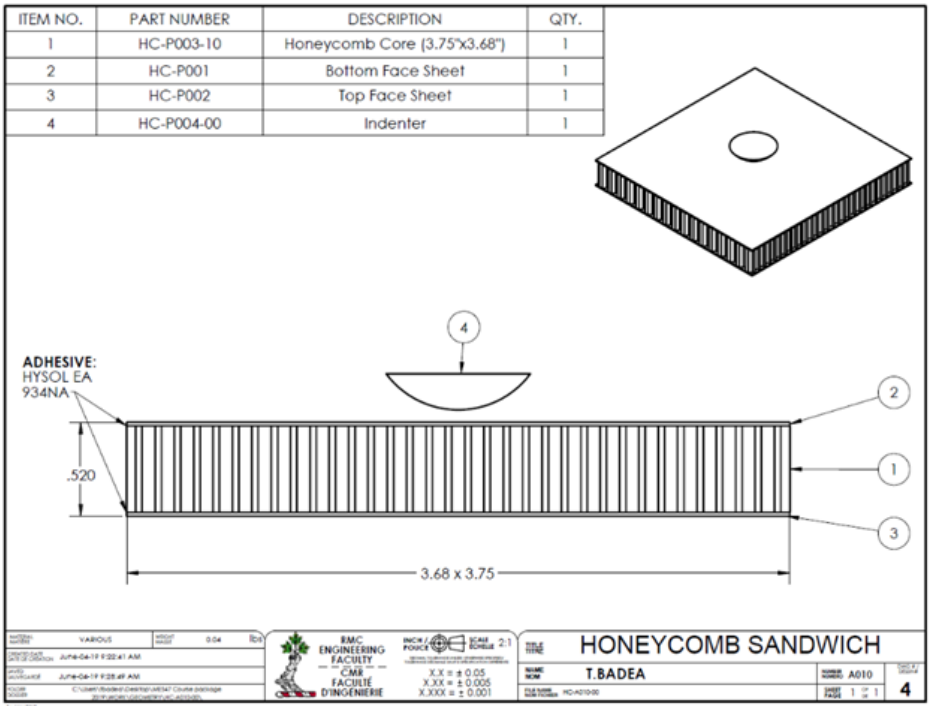

Figure 1: Coupon geometry used to simulate the low velocity impact and compression-after-impact analysis.

Table 1: Material properties of components in model.

Material Variables	5052-H34 Al Core	7075-T6 Al Sheets
Density [kg m^-3]	2680	2810
Elastic Modulus [GPa]	70.3	71.7
Poisson's ratio	0.33	0.33
Yield Strength [MPa]	193	503
Tangent Modulus [MPa]	298.5	670

Stage 2 represents in-plane compression of the dented panel and the boundary conditions are shown in Figure 2.

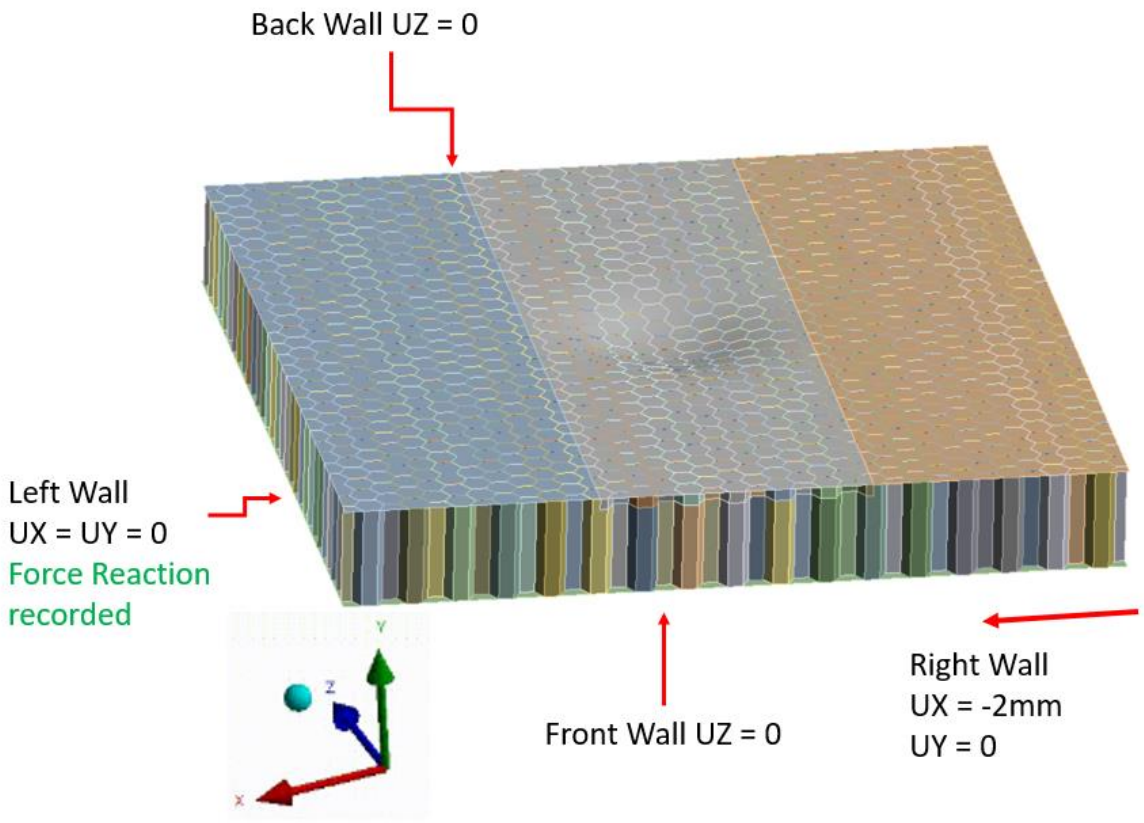

Figure 2: Modeling of the in-plane compression loading and boundary conditions for Stage 2 simulation.

The left wall of the structure is constrained in the X and Y axes while the right wall is used to compress the panel by 2 mm. The front and back walls have symmetry conditions which constrain the displacement of the nodes in the Z direction. The force reaction was recorded at the left wall and plotted against the right wall's displacement during compression to output a force-displacement graph, in order to extract the peak force from the force-displacement graph.

Additional assumptions made in the finite element analysis of the two stages include, the core being perfectly bonded to the face sheets, adhesive representation at the interface of core and face sheet, uniformity of the bonded area and no delamination or core cracking during the impact.

Verifying whether the residual stresses have an effect on the residual strength of the panel is done by comparing a simulation which includes the stresses in the dented facesheet and crumpled core to one where the residual stresses have been removed. To do this, both Stage 1 and Stage 2 were carried out in a single simulation and compared to the compression-after-impact (CAI) analysis with the residual stresses removed. Figure 3 shows a diagram of the set-up.

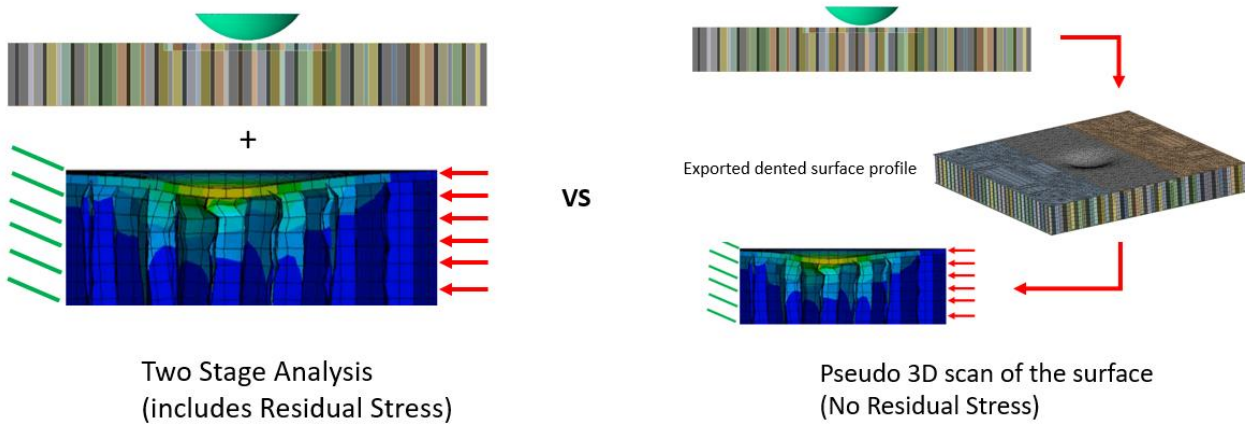

Figure 3: Comparison approach for the consideration of residual stresses in the structure post-impact. Left: Two stage analysis which incorporates both impact and CAI in a single simulation. Right: Exporting of the impacted surface profile and input into separate stage 2 (CAI) analysis.

Exporting the dented surface profile will clear the geometry of any stress information, thus running the simulation without residual stresses post-impact.

Results

The residual compressive strength of a structure can be characterized by the peak force before localization when compressed in the presence of impact damage. When considering the two stage analysis (including residual stresses), plotting the force-displacement curve yields Figure 4.

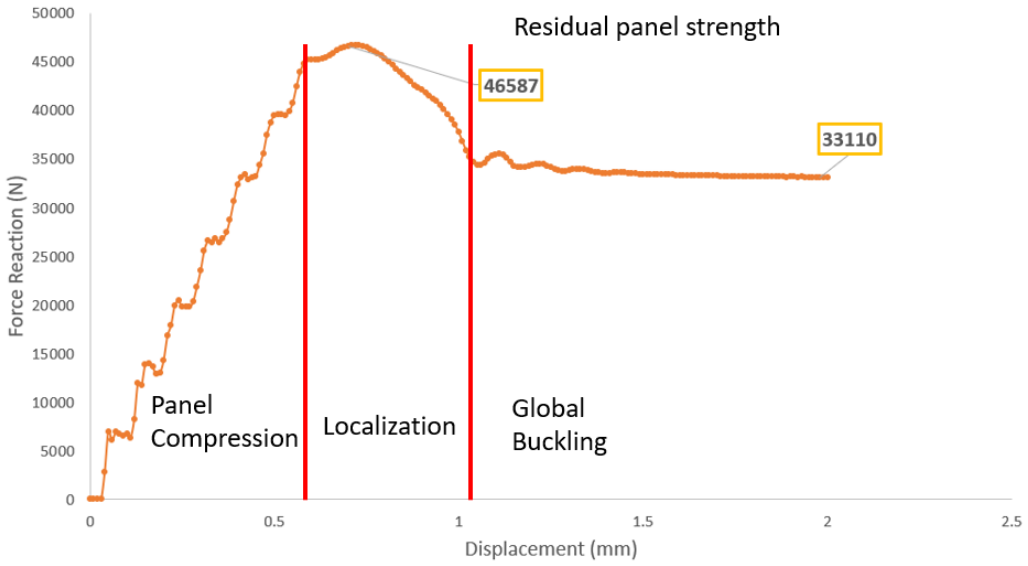

Figure 4: Force-Displacement curve of the analysis including residual stresses.

The peak compressive force in the panel can be seen at the top of Figure 4 to be 46587N at a displacement of 0.7 mm. As the panel is compressed, the force reaction increases linearly up until the

peak force. Localization of the damage reduces the load carrying capacity of the panel until the instability extends to the edges of the panel and global buckling occurs.

Overlaying the force-displacement curve which does not contain residual stresses onto the original curve in Figure 4, will show the difference in force-displacement with and without residual stresses.

Figure 5 compares the force-displacement curves for the simulations with and without residual stresses.

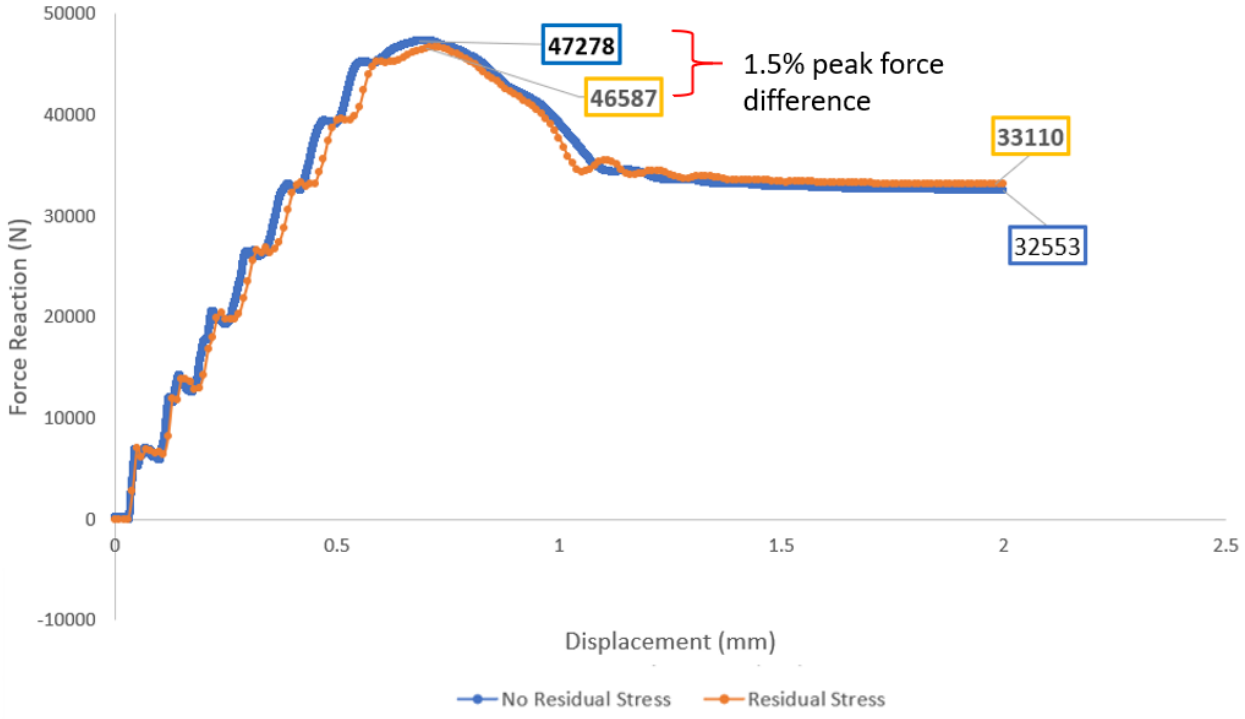

Figure 5: Overlaid force displacement curves of the compression stage with and without residual stresses.

Comparison between the two curves shows a 1.5% difference in the peak force. This enables the conclusion that the residual stresses formed in the dent region have a negligible effect on the peak force. This implies that it is the geometry of the damaged region that is the main driving factor behind the compressive residual strength in the panel. Figures 6 and 7 show the equivalent stress (MPa) throughout the simulations with and without residual stresses. The equivalent stresses are taken from the top facesheet as maximum values anywhere in the dent region.

When looking at the equivalent stress in the panel for both simulations with and without residual stresses, Region B of Figure 6 shows the residual stress in the dented facesheet. One would expect the 450 MPa stresses in the structure to have a significant effect on the peak force sustained by the panel. However, the opposite is true, as region C of Figure 6 shows that for the simulation without residual stresses, the compressive loading causes the stress in the facesheet to quickly rise to 500 MPa (yield stress of the 7075-T6 face sheet). At this point, the stresses for both simulations with and without residual stresses are the same, and continue this way until the end of the simulation.

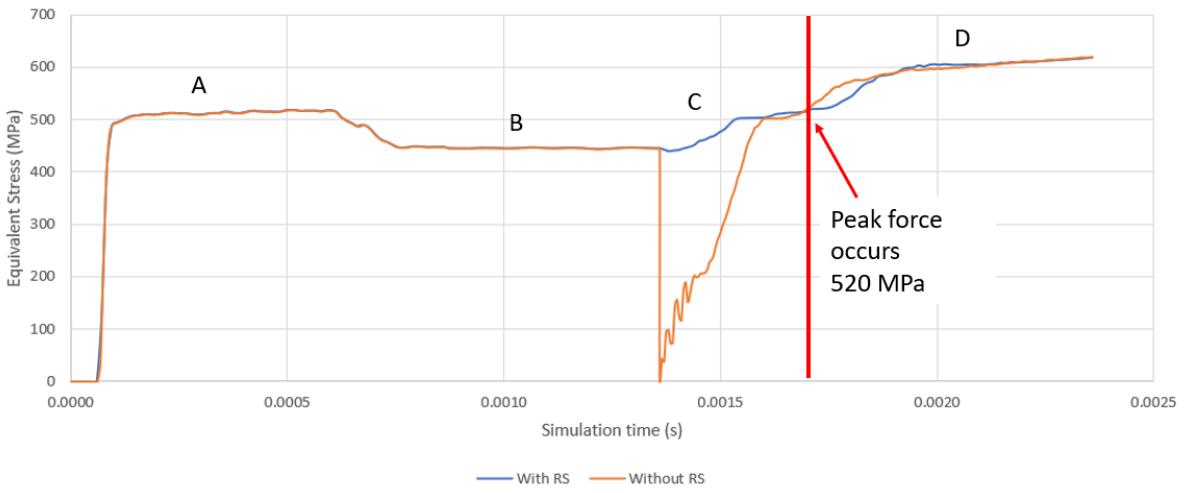

Figure 6: Comparison between simulations with and without Residual Stress (RS) with respect to equivalent stress vs. Simulation time (s).

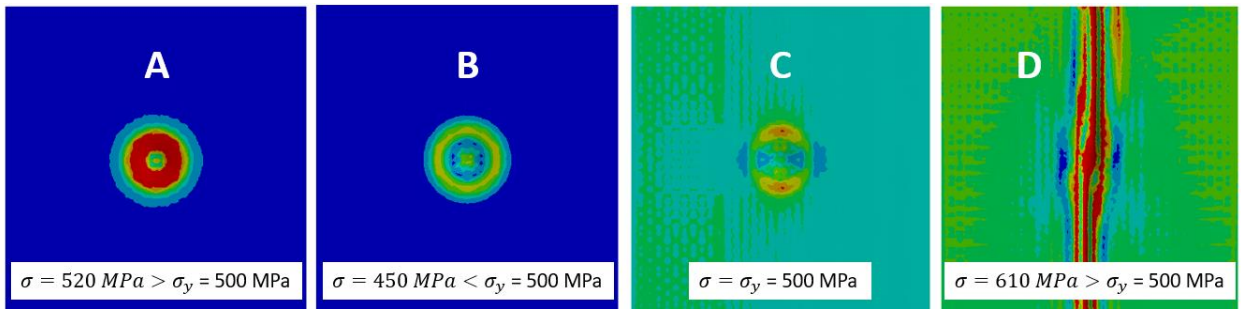

Figure 7: Top View of the stress contours and equivalent stresses in the face sheet, corresponding to the different stages (A-D) in Figure 6. Red indicates equivalent stress above the yield stress of 500MPa.

Figure 8 shows a graph that represents the behavior of the dented face sheet by way of tracked indentation depth (in blue) from the formation of the dent to the global instability. What is interesting to note is that once the compressive loading is applied, the indentation depth starts to increase, and then increases even more significantly as soon as the peak force is recorded.

Figure 8: Indentation depth (blue) and Equivalent stress (orange) curves versus panel displacement during compression, for the simulation with no residual stress.

Figure 9 displays the deepening of the groove and its relation to the peak force, which shows that the stress starts to increase more after the peak force is reached.

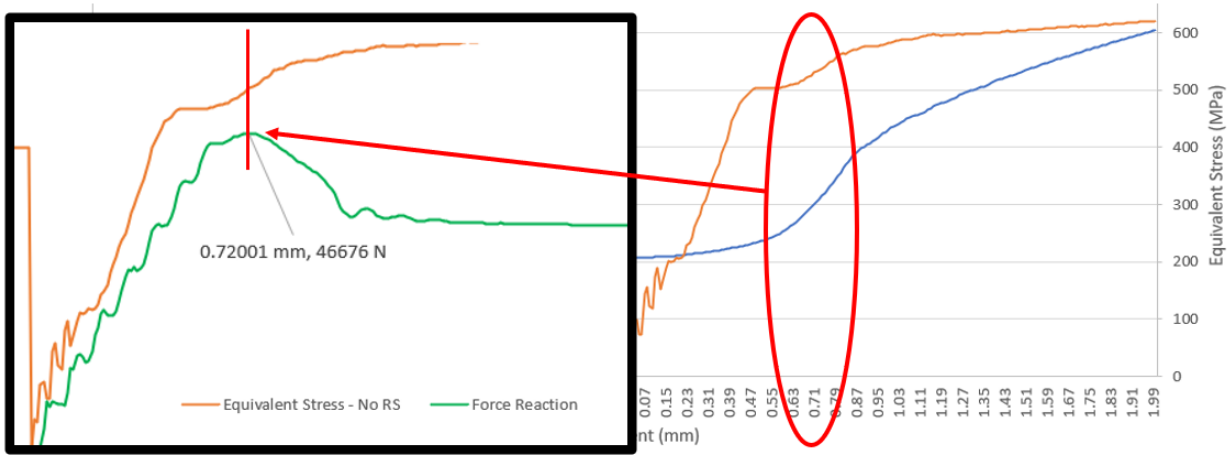

Figure 9: Peak Force occurring due to the groove deepening during CAI.

As the panel is compressed, the facesheet is pushed deeper into the core which causes the core to crush further. After sufficient bending of the facesheet, it can no longer resist the increasing compressive force and a local instability is formed as indicated by decreasing force but increasing indentation depth and stress.

Conclusion

Preliminary results show that the residual stresses in the dented facesheet and the crushed core are not significant contributing factors to the residual compressive strength of the panel with only a 1.5% difference in peak force predicted. Preliminary work has also shown that, the same conclusion is reached when considering different dent depths. This implies that the geometry of the dent is the main driving force behind predicting the residual compressive strength. This has the potential to allow a 3D scan of the surface profile and a crumpled core representation to predict the panel's residual compressive strength.

Future work includes running multiple parameter variations to support these conclusions for different dent shapes and core configurations, experimentally validating these compression-after-impact studies, 3D scanning dented panels whereby the aforementioned methodology is utilized to predict the residual compressive strength and further simplifying the simulations to incorporate a representative core damage model.

References

[1] D. McGowan, D. Ambur, "Compression Response of a Sandwich Fuselage Keel Panel With and Without Damage", NASA, Feb 1997, Technical Memorandum 110302

[2] A. Gilloli, C. Sbarufatti, A. Manes, M. Giglio, "Compression After Impact test (CAI) on Nomex honeycomb sandwich panels with thin aluminum skins", Composites Part B: Engineering, 2014, Vol. 67, Pages 313-325

[3] Davies, G.A.O. & Hitchings, D. & Besant, T. & Clarke, A. & Morgan, "Compression after impact strength of composite sandwich panels", Composite Structures, 2004, Vol. 63, pages 1-9

[4] Shyprykevich P, Tomblin J, Ilcewicz L, Vizzini A J, Lacy TE, and Hwang Y. Guidelines for Analysis, Testing, and Nondestructive Inspection of Impact-Damaged Composite Sandwich Structures. DOT/FAA/AR-02/121, 2003.

[5] Krishnan, Arun & Seneviratne, Waruna & Perera, Shenal, "Validation of Compression-after-Impact Experiments Using ABAQUS Simulations", American Society for Composites, 2018

[6] W. Zhao, Z. Xie, X. Li, X. Yue, J. Sun, "Compression after Impact behavior of titanium honeycomb sandwich structures", Journal of Sandwich Structures & Materials, 2018, Vol. 20, Issue 8, pages 639-657